Chapter 3

mRNA display selection of a high-affinity, modification-specific phospho-IκBα-binding fibronectin

Abstract

The complexity of the proteome is greatly expanded by post translational modifications which may generate only minor changes in the physiochemical properties of proteins. Creation of modification-specific affinity reagents that discriminate between different protein states is an important goal of proteomics research. Using a library based on the fibronectin type III domain, we employ *in vitro* selection by mRNA display to generate binders specific to IκBα phosphorylated at serines 32 and 36. The selection yielded one fibronectin molecule, 10C17C25, that binds a phospho-IκBα peptide with a Kd = 18 nM and is over 1000-fold specific compared to the non-phosphorylated peptide. 10C17C25 specifically recognizes wild type, full-length, phosphorylated IκBα from mammalian cell extract and is functional *in vivo*. We also demonstrate the utility of this domain for detection of IKK activity by incorporating it in a FRET sensor, the first application of a designed modification-specific adaptor for FRET sensor design.

While the human genome contains less than 25,000 genes, the proteome contains over one million different proteins when alternative splicing and post translational modifications (PTM) are taken into account (*1*). Post translational modifications are essential to cellular signaling, and the ability to detect and quantitate modifications is challenging but immensely valuable. Nucleic acid based microarrays are powerful proteomic tools, although they cannot detect the presence and extent of PTMs and may not be accurate predictors of protein quantities (*2*). Attempts to generate open-access resources for modification-specific affinity reagents to all proteins are currently under way (*3*). In addition to detection *in vitro*, novel protein affinity reagents that are functional in the intracellular environment are also useful for determining protein localization and for assessing protein function (*4*). Compared to gene and transcript knock-out techniques, domain and state-specific protein binders that knock-down activity may be better determinants of protein function (*5*). Increasingly, *in vitro* selection techniques such as ribosome display and mRNA display are being implemented to generate novel protein-based affinity reagents with alternative scaffolds (*6-8*). Non-immunoglobulin scaffolds that lack disulfides such as the ankyrin-based "DARPins" (*9*) and fibronectin type III "monobodies" (*10*) have advantages over antibodies for both *in vitro* and *in vivo* applications.

Intrinsically unstructured domains compose a large fraction of the proteome, and many are subjected to PTM. An example of such a domain is the N-terminus of IκB. In the classical NF-κB pathway, three IκB proteins, IκBα, β, and ε, regulate the activity of the ubiquitous transcription factor NF-κB (*11*). NF-κB plays an important role in inflammation and is implicated in autoimmune disease and cancer (*12*). Upon

stimulation, IκB kinase (IKK) immediately phosphorylates IκBα at serines 32 and 36 (*13, 14*). IκBα is then ubiquitinated by the SCF-βTrCP E3 ligase complex and degraded by the proteasome, thereby freeing NF-κB to direct transcription (*15*). Reagents that detect or inhibit the degradation of IκBα *in vivo* may be useful in order to understand the many complex pathways to NF-κB activation. Inhibition at this control point is ideal since the functions of IKK and βTrCP are not specific to the classical NF-κB pathway (*12, 16*).

We employed *in vitro* selection by mRNA display to generate novel protein affinity reagents that recognize phosphorylated IκBα specifically. We utilized a combinatorial protein library based on the 10^{th} fibronectin type III domain of human fibronectin (10FnIII) to generate protein molecules that are functional both *in vitro* and *in vivo* (*17*). The target used for this selection was a synthetic phospho-peptide corresponding to amino acid residues 22-41 of human IκBα. This peptide contains the E3 ligase recognition sequence including phosphorylated serines 32 and 36, which are essential for degradation. The target peptide contained an N-terminal biotin spaced by aminohexanoic acid for specific immobilization to either neutravidin agarose or streptavidin acrylamide beads.

The first round of selection was carried out so that the first affinity enrichment step contained at least 3 copies of the 30-trillion member 10FnIII library (*18*). Enrichment was monitored by measuring radiolabeled fusion binding (Figure 3.1, panel a). In order to reduce the enrichment of bead binders, a negative selection step was employed at round 6. After 10 rounds of selection, pool 10 was determined to have approximately 50% binding efficiency at room temperature with relatively low

background binding (1%). Figure 3.1 (panel b) demonstrates that pool 10 binding is both sequence-specific and phospho-specific. Binding to a non-phosphorylated IκBα peptide otherwise identical to the target was equal to background. Likewise, phospho-serines alone are not sufficient for binding. No binding is detected above background to a peptide corresponding to Elk1 residues 380-394 containing two phosphorylated serines.

Pool 10 was cloned, and eleven sequences were obtained. All 11 sequences were highly similar, suggesting that all sequences share a common ancestor (see supporting information). One representative sequence, 10C17, is illustrated in Figure 3.2, panel a. Essentially, only one solution to the molecular recognition of phospho-IκBα was obtained. This may be due to an intrinsic rarity of binders in the library, as obtaining binders to non-structured targets may be more difficult than obtaining binders to structured targets. Alternatively, this may simply be a result of reaching a bottleneck at some point in the selection.

The ability for the binders to express in bacteria is essential for their utility as affinity reagents. Both 10C17 and another pool 10 clone, 10C19, do not express well in *E. Coli* BL21(DE3) (data not shown). In order to improve the expression of 10C17, solubility was evolved using the GFP reporter screen developed by Waldo et al. (*19*). Some of the sequences obtained from each of the three rounds of evolution performed are listed in Figure 3.2, panel a. The improvement in expression was quantitated by comparing total cell fluorescence of 10C17-GFP variants relative to WT 10FnIII (Figure 3.2, panel b). For the first two rounds of evolution, expression was induced with IPTG for four hours (screen 1). We found that while the initial mutations improved expression, the result of the long induction was that fluorescent aggregates were able to accumulate. This

resulted in obtaining variants that performed better than WT 10FnIII in the assay, but did not express as well. We found that decreasing the length of expression to 1.5 hours improved the sensitivity of the screen (Figure 3.2, panel b, screen 2). In order to ensure that function was retained, binding was measured for each of the variants using SDS PAGE quantitated by autoradiography (Figure 3.2, panel c).

From round one of the evolution, a variant containing two mutations was obtained (A21) which improved both solubility and binding (Figure 3.2). Two sequences were obtained from round two which improved solubility and did not affect binding (B11 and B01). The mutations were combined to produce 10C17B25, which displays an additive improvement in solubility. The third round of evolution again generated two variants with both improved expression (C21 and C22). These two mutations were combined to produce 10C17C25, which binds with approximately 94% efficiency (Figure 3.2, panels a, c). This variant was able to be expressed at modest levels in bacteria and was purified by Nickel affinity and ion exchange chromatography. Approximately 1 mg of soluble protein was recovered per liter of culture.

Obtaining improvements in both solubility and binding is likely a result of increased stability of the domain. Note that all of the mutations selected are contained in the N-terminus of the domain. This region may be destabilized as a result of the removal of the ninth fibronectin type III domain that precedes 10FnIII in human fibronectin. It is also interesting to note that 6 mutations in total were implemented to obtain the 10C17C25 variant, but only four positions differ from WT 10FnIII. Two mutations were obtained at position V6 (originally alanine in WT 10FnIII), and position A10 reverted back to Threonine (Figure 3.2, panel a). Mutations were also found which improved

solubility but negatively affected function. Variants B16 and C18 are provided as examples.

We next addressed the affinity and specificity of 10C17C25 as well as its ability to bind endogenous phospho-IκBα from human cell culture (Figure 3.3). 10C17C25 was subcloned into a modified pET 21 vector that creates a C-terminal MBP fusion. MBP was used to increase the expression of 10C17C25 and provide an additional affinity purification tag. 10C17C25-MBP fusion was produced at much higher yields, reaching 45 mg per liter of culture. Binding to both the phosphorylated and non-phosphorylated IκBα peptides was measured using a Biacore T100 instrument (Figure 3.3, panels a-b). 10C17C25-MBP binds phospho-IκB-α with a K_d = 18 nM, which is comparable to high affinity antibodies. No binding to the non-phosphorylated peptide was detected even at 28 μM 10C17C25-MBP (Figure 3.3, panel b). Therefore, the specificity of 10C17C25 is greater than 1000-fold.

We next wanted to determine whether 10C17C25 is able to recognize wild type, full-length IκBα specifically in its phosphorylated state. Phospho-IκBα was produced in 293T cells by stimulation with TNF-α and was stabilized by addition of the protease inhibitor calyculin A and the proteasome inhibitor MG132. Both stimulated and unstimulated cells were lysed with TBS plus 1% triton x-100. 10C17C25-MBP was added to the cleared lysates and incubated with Nickel-NTA beads. Western blot was performed to detect the presence of IκBα using a polyclonal antibody. Figure 3.3 (panel c) demonstrates that 10C17C25 is able to bind full-length IκBα only from TNF-α stimulated cells. The IκBα that is bound by 10C17C25 has a noticeable reduction in mobility typical of phosphorylated IκBα (*13*).

We also tested the ability of 10C17C25 to express and function in the intracellular environment. 10C17C25 was cloned into a modified pIRES-puro vector containing a C-terminal GFP. This fusion protein was well-expressed throughout the cytoplasm and nucleus of 293T cells when transiently transfected. The original selected binder, 10C17-GFP, was also tested in 293T cells, but was found to form dense aggregates and was not diffusely expressed (data not shown). 10C17C25-GFP is able to stabilize phospho-IκBα *in vivo* when transiently expressed likely by blocking and inhibiting the ubiquitin E3 ligase (Figure 3.3, panel d). Only in cells expressing 10C17C25-GFP is the lower mobility band present, which persists even after 30 minutes of TNF-α incubation when IκBα degradation is maximal in 293T cells. This band was also confirmed to be phosphorylated IκBα by western blot with a monoclonal phospho(S32/S36)-specific anti-IκBα antibody (data not shown).

FRET sensors have been employed to detect PTMs reversibly *in vivo* in a spatial and temporal manner (*20*-*22*). The sensors previously developed utilize natural modification-specific binding domains such as SH2 and a chromodomain. These sensors contain an enzyme substrate sequence that is bound by the proximal binding domain upon modification when signaling is active. This binding restrains the sensor, resulting in a change in FRET between an N-terminal CFP and a C-terminal YFP. The potential for such sensors can be greatly expanded by applying *in vitro* selection to create novel modification-specific binding domains. We demonstrated this by creating a FRET-based sensor for IKK activity and assessed its function *in vitro*. The IKK FRET sensor (Figure 3.4, panel a) is similar to FRET sensors used previously. CFP, YFP, and a new multiple cloning site that contains a flexible linker sequence were cloned into a pET21 $(His)_6$-tag

vector (see supporting information). 10C17C25 and a Klenow product encoding IκBα residues 22-41 were cloned into the vector in two orientations with short and long linkers (Figure 3.4, panel b). The second orientation (IKK FS C25 2S and 2L) contains longer linkers than the first (IKK FS C25 1S and 1L) due to the location of the binding surface relative to the termini of the fibronectin domain. A non-selected fibronectin variant was also cloned into one orientation as a control (IKK FS Fn04 control).

The 5 constructs were expressed in *E. coli* BL21(DE3) and purified by nickel-NTA affinity chromatography. The constructs were phosphorylated *in vitro* with recombinant IKK-β, and the reactions were terminated by addition of EDTA after one hour. FRET was then measured on constructs with or without incubation with IKK-β (Figure 3.4, panel c). FRET was quantitated by measuring the ratio of the YFP emission intensity and the CFP emission intensity after excitation at $\lambda = 435$ nm and is represented as a percent change after incubation with kinase (Figure 3.4, panel b). The first orientation results in a small decrease in FRET after IKK-β incubation, while the second orientation results in a substantial increase in FRET. The length of the linker does not significantly affect the change in FRET. Phosphorylation of the control sensor does not result in a change in FRET. This indicates that neither phosphorylation alone nor interaction with IKK-β can account for the changes in FRET observed with IKK FS C25 2S and 2L. Likewise, the FRET response is demonstrated to be a result of binding to the phosphorylated IκBα sequence as excess phospho-peptide reduces the FRET response achieved after incubation with kinase (Figure 3.4, panel c). Using a monoclonal phospho(S32/S36)-specific anti-IκBα antibody, western blot was done to demonstrate that the kinase reaction is efficient and phosphorylation does occur (Figure 3.4, panel d).

In conclusion, we have demonstrated the utility of mRNA display using a combinatorial protein library based on the 10FnIII scaffold for modification-specific recognition of protein domains. We have demonstrated that the selection, combined with solubility evolution, was able to produce a high-affinity, high-specificity binder to phospho-IκBα. This scaffolded library is ideally suited to discrimination of modifications due to the flexible, continuous ligand binding surface generated by the randomized loops (*17*). We have also demonstrated utility of the library for binding unstructured epitopes with high affinity. 10C17C25 has been demonstrated to not only recognize phospho-IκBα *in vitro*, but is able to bind and inhibit degradation *in vivo*. This intracellular inhibition may prove useful for studying the complex NF-κB pathway as an alternative to gene knock-out or overexpression of modified IκB.

Experimental Procedures

Reagents

Oligonucleotides were synthesized by IDT or the Yale Keck oligonucleotide synthesis facility. Oligonucleotide sequences are listed in supporting information. Peptides were synthesized by Biomer-Tech and purified by reverse-phase HPLC. Products were confirmed by electrospray mass spectrometry. For plasmid construction and cloning, see supporting information. *E. Coli* BL21(DE3) was purchased from Novagen. 293T cells were provided by Dr. Pin Wang, USC Deptartment of Chemical Engineering. 293T cells were cultured in DMEM (Dulbecco's modified Eagle's medium) plus 10% fetal bovine serum (Invitrogen).

Selection

The library used in this selection was previously described (*17*). Protein-mRNA fusions were generated as previously described (*18*). Briefly, each round of selection includes PCR, *in vitro* transcription, splint mediated ligation to a 3' puromycin-containing DNA linker (T4 DNA ligase, NEB), urea PAGE purification, reticulocyte lysate translation (Red Nova, Novagen), salt induced fusion formation, oligo-dT cellulose purification (NEB), reverse transcription (Superscript II, Invitrogen), and affinity enrichment. For the first round of selection, the 30 trillion member library was generated with at least 3 copies of fusions going into the affinity enrichment step. Neutravidin agarose or streptavidin ultralink beads (Pierce) were used to display peptides for binding. The selection buffer included PBS supplemented with 0.5 mg/ml BSA (Sigma), 0.1 mg/ml sheared salmon sperm DNA (Sigma), 0.02% Tween 20, and 1 mM DTT. A negative selection step was performed beginning at round 6 following reverse transcription by flowing fusions over empty, blocked beads in column format. Free neutravidin or streptavidin (Pierce) was also including in the selection binding buffer to compete with background binders. Binding was measured by scintillation counting of ^{35}S-Methionine labeled, oligo-dT cellulose purified fusions. All binding and washing was performed at room temperature. Pool 10 was cloned into a TOPO-TA vector (Invitrogen) for sequencing.

Solubility evolution

The GFP reporter screen and fluorescence quantitation was carried out as previously described (*17, 19*). Error prone PCR was performed with 7 mM $MgCl_2$ and 0.05 mM

$MnCl_2$ to generate one to two mutations per gene. The best clones from each round were sequenced and tested for binding. Crude, ^{35}S-Methionine labeled, *in vitro* translated protein was bound to immobilized target peptide or empty beads, washed, and eluted with SDS PAGE loading buffer. An equivalent amount of crude translation product and eluted protein were analyzed by SDS PAGE autoradiography to determine percent protein bound.

Surface plasmon resonance

SPR was performed on a Biacore T100 instrument. Peptides were immobilized on SA chips at 40 RU. 10C17C25-MBP was expressed in *E. Coli* BL21(DE3) by induction with 1 mM IPTG at mid log phase for 3 hours. Pelleted cells were lysed with B-PER (Pierce) and affinity-purified with a nickel-NTA column (Qiagen), followed by affinity purification with an amylose resin column (NEB) and desalting (PD-10, Amersham Biosciences). Biacore buffer includes PBS plus 0.5 mg/ml BSA and 0.05% Tween 20. Various concentrations of analyte were flowed at 100 μl/min for two minutes and allowed to fall off for 45 minutes. Binding sensograms were fitted with Biacore evaluation software.

Pull-down

Confluent cell culture was incubated with TNF-α (20 ng/ml), MG132 (10 μM), and calyculin A (50 nM), respectively, for 15 minutes (Calbiochem). Stimulated and unstimulated cells were lysed for 5 minutes with ice cold lysis buffer (PBS, 1% triton x-100, 20 ng/ml MG132, 100 nM calyculin A, protease inhibitor cocktail III (Calbiochem)

and 1 mM EDTA). MG132 was required during lysis and binding to prevent degradation and depletion of phosphorylated IκBα. Cell extracts were cleared by centrifugation at 20,000 x g for 5 minutes, combined with purified 10C17C25-MBP, and incubated with nickel-NTA beads for one hour at 4ºC. After 3 washes, samples were eluted with PAGE loading buffer. Crude cell extracts from stimulated and unstimulated cells were run with the eluted samples on SDS PAGE (NuPAGE system, Invitrogen), transferred to PVDF membrane (Biorad), and incubated with polyclonal anti-IκBα antibody (Santa Cruz Biotechnology). After secondary antibody incubation, blots were incubated with SuperSignal West Dura substrate (Pierce) and imaged by chemiluminescence with an Alpha Imager equipped with a cooled CCD camera.

In vivo inhibition

293T cells were transiently transfected with 10C17C25-GFP or Fn04-GFP using Lipofectamine Plus reagent (Invitrogen) following the manufacturers recommendations. One day post-transfection, cells were stimulated with 20 ng/ml TNF-α for the indicated time. Crude cell extracts were prepared and analyzed by western blot.

IKK FRET sensor

FRET sensor proteins were expressed as described for 10C17C25-MBP. Nickel-NTA affinity purified sensors (50 μg/ml) were kinased with recombinant IKKβ (1 μg/ml, Invitrogen) in 20 mM Tris, pH 7.5 plus 10 mM magnesium and 200 μM ATP. Reactions were terminated by addition of EDTA. Fluorescence emission spectra were obtained using a Shimadzu fluorimeter RF-5301PC by excitation at 435 nm with 5 nm slit widths.

FRET was calculated as the emission intensity at 525 nm divided by the intensity at 475 nm. Western blot was performed as described using a monoclonal phospho-IκBα antibody (Cell signaling Technology).

References

(1) Jensen, O. N. (2004) Modification-specific proteomics: characterization of post-translational modifications by mass spectrometry. *Curr Opin Chem Biol 8*, 33-41.

(2) Gygi, S. P., Rochon, Y., Franza, B. R., and Aebersold, R. (1999) Correlation between protein and mRNA abundance in yeast. *Mol Cell Biol 19*, 1720-30.

(3) Taussig, M. J., Stoevesandt, O., Borrebaeck, C. A., Bradbury, A. R., Cahill, D., Cambillau, C., de Daruvar, A., Dubel, S., Eichler, J., Frank, R., Gibson, T. J., Gloriam, D., Gold, L., Herberg, F. W., Hermjakob, H., Hoheisel, J. D., Joos, T. O., Kallioniemi, O., Koegl, M., Konthur, Z., Korn, B., Kremmer, E., Krobitsch, S., Landegren, U., van der Maarel, S., McCafferty, J., Muyldermans, S., Nygren, P. A., Palcy, S., Pluckthun, A., Polic, B., Przybylski, M., Saviranta, P., Sawyer, A., Sherman, D. J., Skerra, A., Templin, M., Ueffing, M., and Uhlen, M. (2007) ProteomeBinders: planning a European resource of affinity reagents for analysis of the human proteome. *Nat Methods 4*, 13-7.

(4) Nizak, C., Monier, S., del Nery, E., Moutel, S., Goud, B., and Perez, F. (2003) Recombinant antibodies to the small GTPase Rab6 as conformation sensors. *Science 300*, 984-7.

(5) Stocks, M. (2005) Intrabodies as drug discovery tools and therapeutics. *Curr Opin Chem Biol 9*, 359-65.

(6) Lipovsek, D., and Pluckthun, A. (2004) In-vitro protein evolution by ribosome display and mRNA display. *J Immunol Methods 290*, 51-67.

(7) Roberts, R. W., and Szostak, J. W. (1997) RNA-peptide fusions for the in vitro selection of peptides and proteins. *Proc Natl Acad Sci U S A 94*, 12297-302.

(8) Hanes, J., and Pluckthun, A. (1997) In vitro selection and evolution of functional proteins by using ribosome display. *Proc Natl Acad Sci U S A 94*, 4937-42.

(9) Kawe, M., Forrer, P., Amstutz, P., and Pluckthun, A. (2006) Isolation of intracellular proteinase inhibitors derived from designed ankyrin repeat proteins by genetic screening. *J Biol Chem 281*, 40252-63.

(10) Koide, A., Abbatiello, S., Rothgery, L., and Koide, S. (2002) Probing protein conformational changes in living cells by using designer binding proteins: application to the estrogen receptor. *Proc. Natl. Acad. Sci. USA 99*, 1253-8.

(11) Hoffmann, A., Levchenko, A., Scott, M. L., and Baltimore, D. (2002) The IkappaB-NF-kappaB signaling module: temporal control and selective gene activation. *Science 298*, 1241-5.

(12) Viatour, P., Merville, M. P., Bours, V., and Chariot, A. (2005) Phosphorylation of NF-kappaB and IkappaB proteins: implications in cancer and inflammation. *Trends Biochem Sci 30*, 43-52.

(13) Brown, K., Gerstberger, S., Carlson, L., Franzoso, G., and Siebenlist, U. (1995) Control of I kappa B-alpha proteolysis by site-specific, signal-induced phosphorylation. *Science 267*, 1485-8.

(14) DiDonato, J. A., Hayakawa, M., Rothwarf, D. M., Zandi, E., and Karin, M. (1997) A cytokine-responsive IkappaB kinase that activates the transcription factor NF-kappaB. *Nature 388*, 548-54.

(15) Yaron, A., Hatzubai, A., Davis, M., Lavon, I., Amit, S., Manning, A. M., Andersen, J. S., Mann, M., Mercurio, F., and Ben-Neriah, Y. (1998) Identification of the receptor component of the IkappaBalpha-ubiquitin ligase. *Nature 396*, 590-4.

(16) Fuchs, S. Y., Spiegelman, V. S., and Kumar, K. G. (2004) The many faces of beta-TrCP E3 ubiquitin ligases: reflections in the magic mirror of cancer. *Oncogene 23*, 2028-36.

(17) Olson, C. A., and Roberts, R. W. (2007) Design, expression, and stability of a diverse protein library based on the human fibronectin type III domain. *Protein Sci 16*, 476-84.

(18) Liu, R., Barrick, J. E., Szostak, J. W., and Roberts, R. W. (2000) Optimized synthesis of RNA-protein fusions for in vitro protein selection. *Methods Enzymol 318*, 268-93.

(19) Waldo, G. S., Standish, B. M., Berendzen, J., and Terwilliger, T. C. (1999) Rapid protein-folding assay using green fluorescent protein. *Nat. Biotechnol. 17*, 691-5.

(20) Lin, C. W., Jao, C. Y., and Ting, A. Y. (2004) Genetically encoded fluorescent reporters of histone methylation in living cells. *J Am Chem Soc 126*, 5982-3.

(21) Sato, M., Ozawa, T., Inukai, K., Asano, T., and Umezawa, Y. (2002) Fluorescent indicators for imaging protein phosphorylation in single living cells. *Nat Biotechnol 20*, 287-94.

(22) Wang, Y., Botvinick, E. L., Zhao, Y., Berns, M. W., Usami, S., Tsien, R. Y., and Chien, S. (2005) Visualizing the mechanical activation of Src. *Nature 434*, 1040-5.

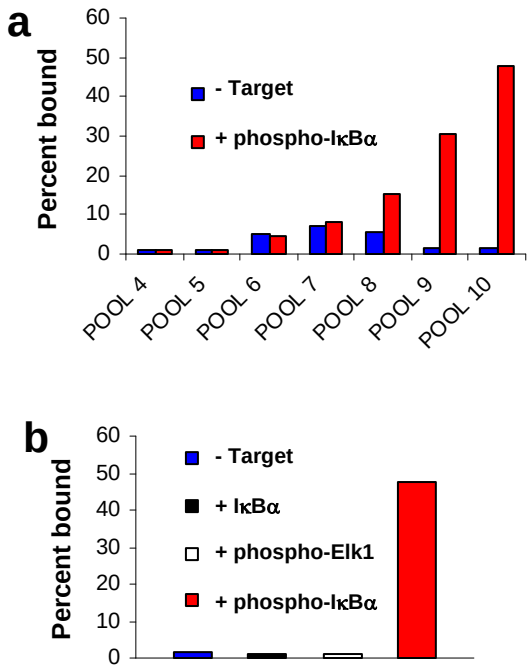

Figure 3.1 Selection of phospho-IκBα binders. a) The enrichment of target binders was monitored by radiolabeled fusion binding assays. b) Pool 10 binding is sequence specific and phospho-specific. Binding to the non-phosphorylated IκBα peptide and a dissimilar phospho-serine peptide is equal to background.

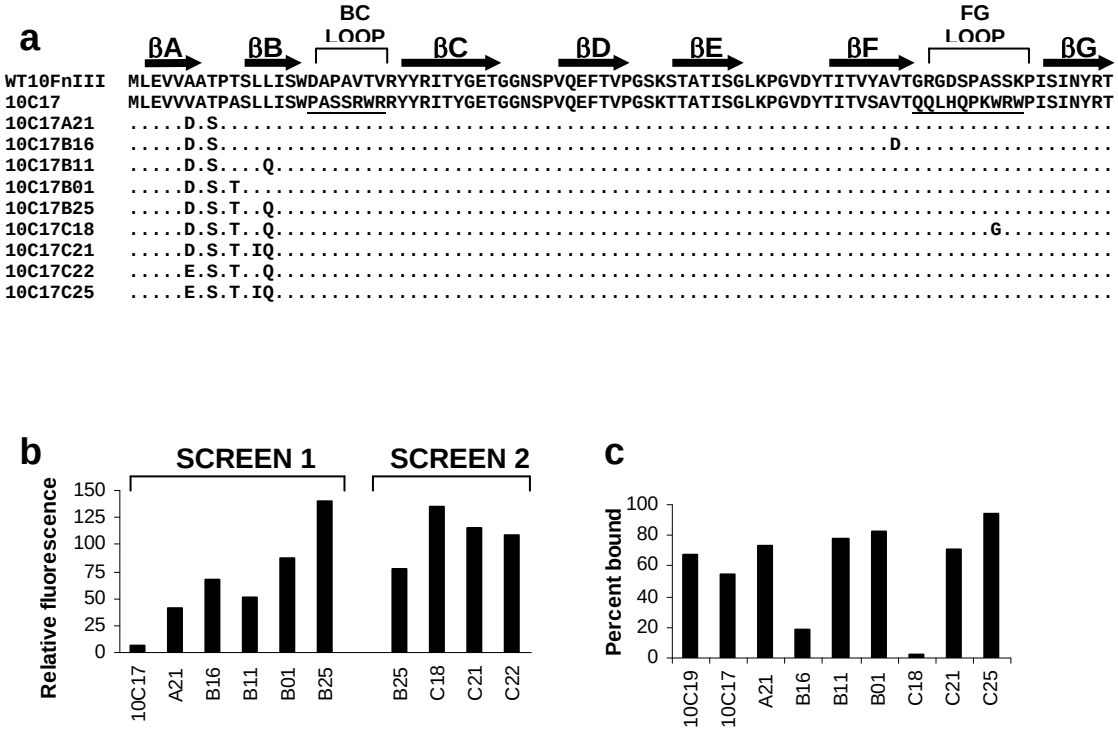

Figure 3.2 Solubility evolution of selection winner using a GFP reporter screen (*19*)**.** a) Sequence of wild type 10FnIII, a pool 10 clone (10C17), and evolved variants of 10C17 from three rounds of evolution. Dots represent sequence identical to 10C17. b) Total cell fluorescence of expression cultures. Proteins were expressed for 4 hours (screen 1) or 1.5 hours (screen 2). c) Binding of selected clones with in vitro translated protein measured by SDS PAGE autoradiography (representative data).

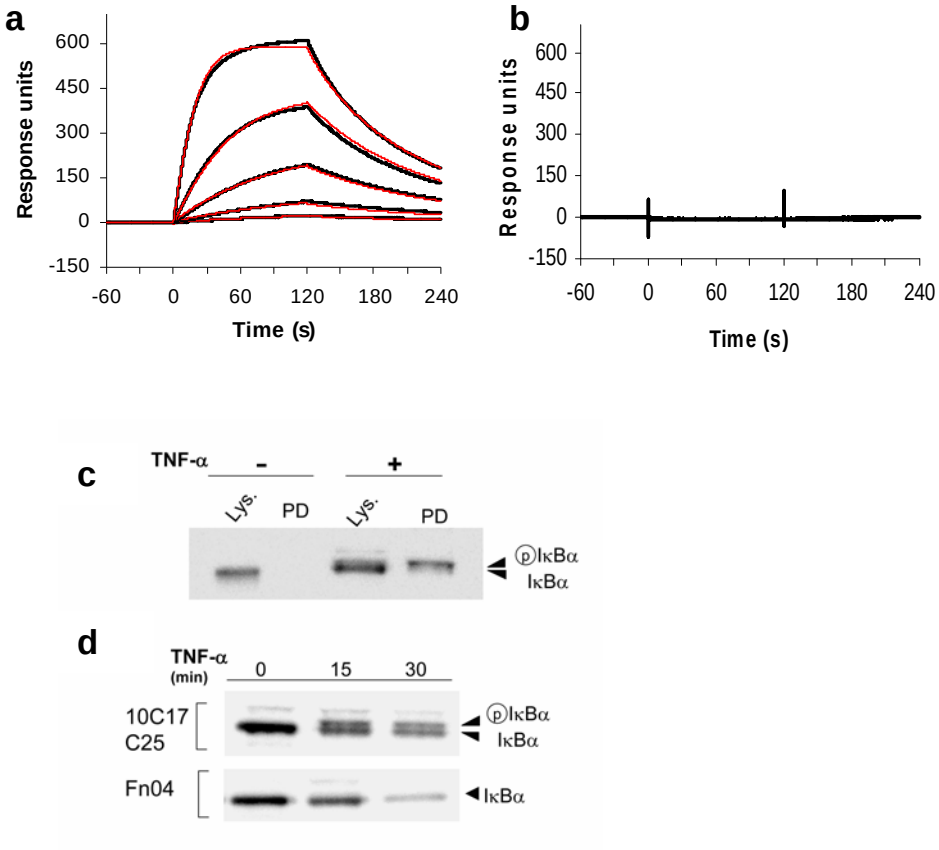

Figure 3.3 Affinity and specificity of 10C17C25. SPR was performed to test affinity and specificity to phospho-IκBα. Concentrations of 10C17C25-MBP ranged from 0.3 nM to 100 nM for phospho-IκBα binding (panel a) and up to 28 μM for non-phosphorylated IκBα peptide binding (panel b). Black represents raw data, red represents curve fits. c) Modification-specific binding to full-length IκBα was determined by pull-down from mammalian cell culture. d) Intracellular function was demonstrated by the inhibition of IκBα degradation in TNF-α stimulated 293T cells transiently transfected with 10C17C25-GFP. Cells transiently transfected with non-selected Fn04-GFP were used as a control.

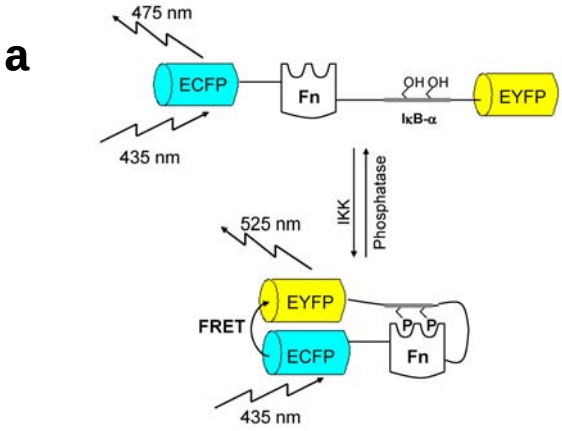

b

	IKK FS	Δ FRET (%)
CFP – IκBα – Ln9 – Fn – YFP	C25 1S	-15
CFP – IκBα – Ln19 – Fn – YFP	C25 1L	-8.3
CFP – Fn – Ln15 – IκBα – YFP	C25 2S	47
CFP – Fn – Ln25 – IκBα – YFP	C25 2L	51
CFP – Fn – Ln15 – IκBα – YFP	Fn04 Control	-0.1

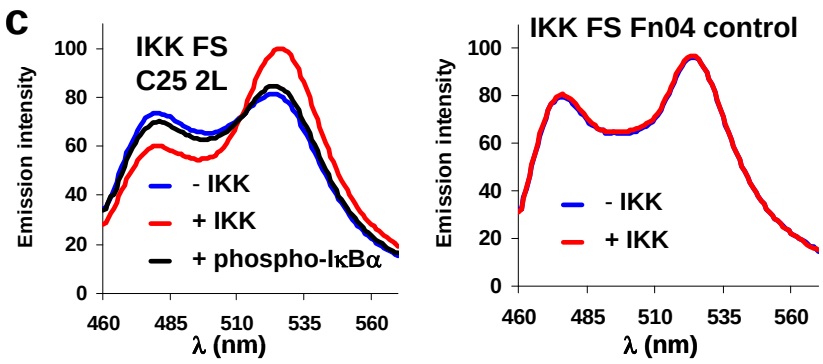

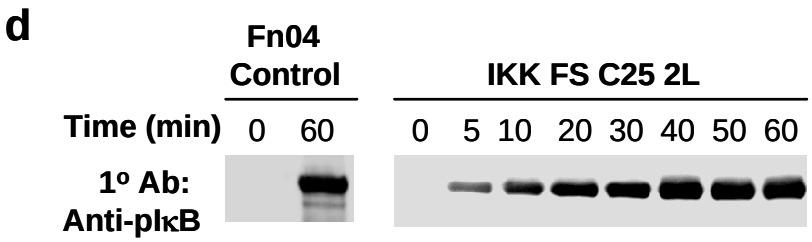

Figure 4.4 IKK FRET sensor. See caption on following page.

Figure 4.4 IKK FRET sensor. a) Illustration of a FRET sensor for IKK activity using a designed modification-specific fibronectin binder. b) Four sensors were created as well as a control containing non-selected Fn04. The IKK substrate sequence includes IκBα residues 23-41. Constructs containing the kinase substrate N-terminal to 10C17C25 resulted in a slight decrease in FRET upon phosphorylation. Constructs containing the substrate sequence C-terminal to 10C17C25 resulted in a large increase in FRET upon phosphorylation. c) Representative fluorescence emission spectra of IKK FRET sensors. Excess phosphorylated IκBα peptide was able to largely eliminate the FRET gained after phosphorylation. d) The kinase reaction was demonstrated to be efficient by western blot using a phospho-specific monoclonal antibody.

Supporting Information

All oligonucleotides were purchased from Integrated DNA Technologies unless otherwise stated. All oligos longer than 35 nucleotides were purified by urea PAGE. Fnoligo1 and Fnoligo8 were used for amplification during selection.

Fnoligo1: 5′-TTCTAATACGACTCACTATAGGGACAATTACTATTTACAATTA-
CAATGCTCGAGGTCGTCG

Fnoligo8: 5′-GGAGCCGCTACCGGATCCGGTGCGGTAGTTGATGGAGATCGG

Fnoligo1 contains the T7 RNA polymerase promoter sequence, a portion of the TMV translation enhancer sequence, and anneals to the 5’ end of the Fn library. Fnoligo8 anneals to the 3’ end of the Fn library, contains a BamHI restriction site, and codes for a $(Gly\text{-}Ser)_3$ spacer. After *in vitro* transcription, mRNA pools were ligated to pF30P (Yale Keck Oligonucleotide synthesis facility) using Fn-pF30P-Splint.

pF30P: 5′-phospho-A_{21}-9_3-ACC-Pu, 9 = phosphoramidite spacer 9, Pu = Puromycin (Glen Research)

Fn-pF30P-Splint: 5′-TTTTTTTTTTTTGGAGCCGCTACC

The pool 10 PCR product was cloned into pCR4-TOPO TA cloning vector (Invitrogen). Eleven sequences were obtained:

Pool 10 sequences:

```
WT10FnIII  MLEVVAATPTSLLISWDAPAVTVRYYRITYGETGGNSPVQEFTVPGSKSTATISGLKPGVDYTITVYAVTGRGDSPASSKPISINYRT
FnIkB10C19 ................PASSRWR.............................................QQLRQPKWRW........
FnIkB10C08 ................PASSRWR.............................................L.QQLRQPKWRW........
FnIkB10C04 ................PTSSRWR.............................................QQLRQPKWRW........
FnIkB10C03 ................PASSRWR.........................................C...QQLHQPKWRW........
FnIkB10C05 ................PASSRWR............G...K.........................C...QQLHQPKWRW........
FnIkB10C16 ................PASSRWR.........................................C...QQLHQPKWRW........
FnIkB10C18 ................PASSRWR.............................R.........C...QQLHQPKWRW........
FnIkB10C20 ................PASSRWR......C...D.....R.........................C...QQLHQPKWRW........
FnIkB10C01 ............Q...PASSRWRH.....................................C...QQLHQPKWRW........
FnIkB10C09 .....V..........PASSRWR.....................................C...QQLHQPKWRW........
FnIkB10C17 .....V...A......PASSRWR.....................T...............S...QQLHQPKWRW........
```

Fnoligo1 and Fnoligo8 were used to amplify 10C17 and 10C19 for *in vitro* transcription, followed by *in vitro* translation to determine binding efficiencies.

All restriction enzymes and T4 DNA ligase were purchased from NEB. 10C17 and 10C19 were amplified with primers “Fnlibrary5Nhe” and “Fnlibrary3His” for cloning into pET11a.

```
Fnlibrary5NdeI: 5′-CTATTTACAATTCATATGCTCGAGGTCGTCG
Fnlibrary3His: 5′-GGTTGGTGATCAGTGGTGATGGTGGTGATGGGATC-
                  CGGTGCGGTAGTTG
```

Fnlibrary5NdeI contains an NdeI digestion sequence and anneals to the 5’ end of the Fn library. Fnlibrary3His anneals to the 3’ end of the Fn library, contains a BamHI restriction site, codes for a $(His)_6$-tag, and contains a BclI restriction site. The PCR products were digested with NdeI and BclI, purified (QIaquick, Qiagen), and were ligated into the NdeI and BamHI restriction sites of pET11a, creating vectors pAO5-10C17 and pAO510C19. Insertion of genes into the NdeI and BamHI restriction sites of the new pAO5 vectors will result in addition of a C-terminal $(His)_6$-tag, immediately followed by a stop codon (see Appendix A). pAO5-10C17 and pAO5-10C19 were expressed in *E. Coli* BL21(DE3) but did not produce detectable soluble protein. 10C17-$(His)_6$ was purified under denaturing conditions, but attempts to refold the protein were unsuccessful.

10C17 and subsequent variants were amplified under error prone conditions (7 mM $MgCl_2$, 0.05 mM $MnCl_2$) using Fnlibrary5NdeI primer and Fnoligo8. The resulting PCR products were digested with NdeI and BamHI and cloned into the GFP-reporter vector generously provided by Dr. Geoffry S. Waldo. To test binding, selected variants were

amplified with Fnoligo1 and Fnoligo8 for subsequent *in vitro* transcription and translation. 10C17B25 (see Figure 3.2) was created by amplifying 10C17B11 with 10C17oligoA10T, followed by FnoligoNdeI.

`10C17oligoA10T: CATATGCTCGAGGTCGTCGATGCATCTCCAACCAGCCTCCAGATCAGC`

10C17B25 was used as the template for the third round of solubility evolution. 10C17C25 was created by amplifying 10C17C21 with 10C17oligoD6E.

`10C17oligoD6E: GGAGATATACATATGCTCGAGGTCGTCGAAGCATCACCAACCAGC`

The gene inserts from selected clones were digested directly from the minipreped GFP reporter plasmids using NdeI and BamHI, purified by agarose gel electrophoresis (QIAquick, Qiagen), and ligated into the NheI and BamHI sites of pAO5 for expression of C-terminal His-tagged proteins lacking GFP.

In order to increase the yields of soluble 10C17C25, two fusion vectors were created with MBP as an N-terminal (pAO7) or C-terminal fusion (pAO9) (see Appendix A). Both orientations were tested in order to determine if the enhancement in expression mediated by MBP is dependent on fusion orientation. pAO5-10C17C25 plasmid was digested with either XhoI and BamHI or NdeI and BamHI, and the 10C17C25 fragments were agarose gel purified. These fragments were ligated into purified pAO7 or pAO9 digested with XhoI and BamHI or NdeI and BamHI, respectively. We found that the orientation of the MBP fusion does not affect the amount of soluble protein expressed and chose pAO9-10C17C25 for large-scale expression.

For mammalian cell culture expression, 10C17C25-GFP was amplified in two steps (from the GFP reporter vector) with Fn5pIRES and GFP3FLAG1, followed by amplification with Fn5pIRES and GFP3FLAG2.

`Fn5pIRES: 5′-CTTCTAGCGGCCGCCACCATGCTCGAGGTCGTCG`

GFP3FLAG1: 5′-CGTCCTTGTAGTCACCAGAGCCTTTGTAGAGCTCATCCATGCCATGTG

GFP3FLAG2: 5′-GTGACCTGATCACTTATCGTCATCGTCCTTGTAGTCACCAGAGC

Fn5pIRES contains a Not I restriction site, encodes a Kozak sequence, and anneals to the 5’ end of the Fn library. GFP3FLAG1 anneals to the 3’ end of GPF and encodes a Flag sequence. GFP3FLAG2 extends the Flag sequence and adds a BclI restriction site. The PCR products were digested with NotI and BclI and cloned into the NotI and BamHI sites of pIRESpuro (Clontech).

In order to create a new FRET sensor vector with a versatile multiple cloning site, we constructed pKC1 (see Appendix A). The oligos used to create the IKK FRET sensors are:

IKK1F: 5′-GGTTGGAAGCTTGGAGCGTCTGCTCGACGATCGCCATGACAGCGGACTGG

IKK1R: 5′-GGTGGTCGGCCGATTCCTCATCCTTCATAGAATCCAGTCCGCTGTCATGG

IKK2F: 5′-GGTGGTCTCGAGCGGAAGCAACGGTGGAAGCGAGCGTCTGCTCGACGA-
TCGCCATGACAGC

IKK2R: 5′-GGTGGTGGATCCAGATTCCTCATCCTTCATAGAATCCAGTCCGCTGT-
CATGGCGATCGTCG

C25XhoI5S: 5′-GGTGGTCTCGAGCATGCTGGAGGTCGTCGAAGCATC

C25XhoI5L: 5′-GGTGGTCTCGAGCGGAAGCAACGGTGGAAGCAACGGGTCGTCT-
ATGCTGGAGGTCGTCGAAGC

C25HindIII5: 5′-GGTTGGAAGCTTGGGCGGTATGCTCGAGGTCGTCGAAGC

FnHindIII5: 5′- GGTTGGAAGCTTGGGCGGTATGCTCGAGGTCGTCGCTGC

FnEagI3S: 5′- GGTGGTCGGCCGAGGTGCGGTAGTTGATGGAGATCG

FnEagI3L: 5′- GGTGGTCGGCCGACCCGTTGCTTCCACCGTTGCTTCCG-
CTAGAGGTGCGGTAGTTGATGGAGATCG

First, the IKK substrate sequences were assembled by extending either IKK1F and IKK1R or IKK2F and IKK2R with Klenow Fragment (3’→5’ exo-) per the

manufacturer's instructions (NEB). To create IKK FS C25 1S and 1L, the IKK1 fragment was digested with HindIII and EagI and ligated into the HindIII and EagI restriction sites of pKC1. To create IKK FS C25 2S and 2L, the IKK2 fragment was digested with XhoI and BamHI and ligated into the XhoI and BamHI sites of pKC1. 10C17C25 was amplified with either C25XhoI5S and Fnoligo8 or C25XhoI5L and Fnoligo8. Both PCR products were digested with XhoI and BamHI and ligated into pKC1 containing the IKK1 substrate sequence to create IKK FS C25 1S and 1L (See Figure 3.4b). 10C17C25 was next amplified with either C25HindIII and FnEagI3S or C25HindIII and FnEagI3L. A non-selected control, Fn04, was also amplified with FnHindIII5 and FnEagI3S. All three PCR products were digested with HindIII and EagI and ligated into pKC1 containing the IKK2 substrate sequence to create IKK FS C25 2S, 2L and control FS Fn04. The linker sequences for the five constructs are illustrated below. The underlined sequences are encoded by pKC1.